Silica Nanostructures

DOI: 10.1002/ange.200602274

Nanoscale Silica Capsules Ordered on a Substrate: Oxidation of Nanocellular Thin Films of Poly(styrene-*b*-dimethylsiloxane)**

*Lei Li and Hideaki Yokoyama**

The fabrication of nanoscale hollow particles has been receiving increasing attention in both academic and industrial fields. Various materials have been adopted to satisfy the growing needs for encapsulation,[1,2] and a variety of chemical and physicochemical methods have been developed in order to prepare hollow spheres with controlled size and shape, including colloid particle templating,[3] sol–gel synthesis,[4] layer-by-layer self-assembly,[5] and surface living polymerization.[6] Block copolymers are considered to be ideal candidates for the fabrication of nanoscale structures, owing to their predictable self-assembly in the size range 5–50 nm.[7,8] Our group recently reported a nondestructive CO_2 foaming method that introduces 15–30-nm voids into CO_2-philic fluorinated block copolymers.[9–12] Herein, we extend the same methodology to poly(styrene-*b*-dimethylsiloxane) (PS-PDMS), the PDMS domain of which is a CO_2-philic polymer,[13] to fabricate nanocells in thin films and to convert them into silica hollow particles (nanocapsules) ordered on substrates by oxidation.[14] Silica nanocapsules with a number density of $7.0 \times 10^{10}\,cm^{-2}$, a diameter of less than 40 nm, and a wall thickness of 2 nm were successfully synthesized.

We first made a PS-PDMS thin film with a thickness of 43 nm and a single layer of PDMS spherical domains on a silicon wafer. It is well known that PDMS can be easily converted into silica by exposure to UV light/ozone[15] and that PS is totally decomposed under these conditions. The PDMS nanodomains are therefore converted into silica particles, as shown schematically in Figure 1a,b. These particles were found to be spherical with a number density of $8.9 \times 10^{10}\,cm^{-2}$, as observed by atomic force microscopy (AFM; Figure 1c).

The oxidation process was monitored by X-ray photoelectron spectroscopy (XPS). The atomic fractions of C, Si, and O were determined from the intensities of the C1s, Si2p and O1s peaks, respectively, as a function of oxidation time. The Si2p peaks are shown in Figure 2a as an example. A single Si2p peak due to untreated PS-PDMS is found initially

[*] Dr. L. Li, Dr. H. Yokoyama
Nanotechnology Research Institute
National Institute of Advanced Industrial Science and Technology
1-1-1, Higashi, Tsukuba, Ibaraki 305-8565 (Japan)
Fax: (+81) 29-861-4432
E-mail: yokoyama@ni.aist.go.jp

[**] This research was partially funded by the Project on Nanostructured Polymeric Materials of New Energy and Industrial Technology Development Organization. L.L. thanks the Japan Society for the Promotion of Science for a fellowship.

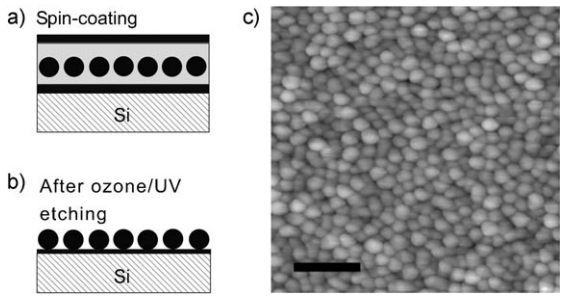

Figure 1. Formation of silica nanodots from a PS-PDMS thin film using UV light/ozone oxidation. a) Morphology of the as-cast PS-PDMS copolymer thin film. Spherical PDMS nanodomains are dispersed in a continuous PS matrix by micro-phase separation. The black and gray domains represent the PDMS and PS domains, respectively. b) The PS domains are decomposed, and the PDMS domains are converted into silica by UV light/ozone oxidation. c) Topographic AFM image of the silica nanodots after oxidation with UV light/ozone for 1 h (scale bar 200 nm).

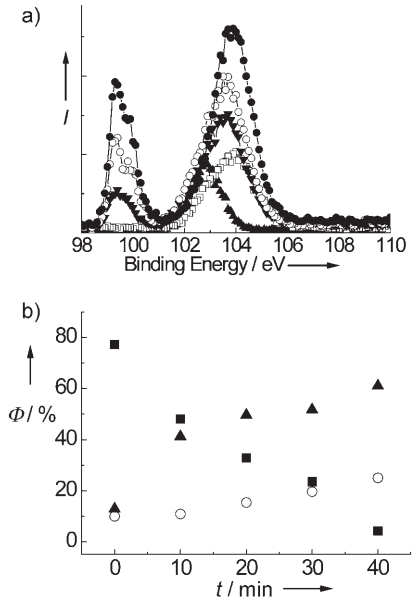

Figure 2. a) Photoelectron intensities, *I*, of the Si2p peaks from the PS-PDMS thin film, after oxidation with UV light/ozone for 0 (▲), 10 (□), 20 (▼), 30 (○), and 40 min (●). b) Atomic fractions, Φ, in the PS-PDMS thin film versus oxidation time, *t*, determined from the C1s (■), Si2p (○), and O1s (▲) XPS peaks. The atomic fraction of oxidized Si can be obtained from the Si2p binding-energy region 101–106 eV.

at 102.6 eV. This peak shifts to 104 eV after oxidation for 10 min with UV light/ozone, thereby indicating formation of silicon oxide.[16] After etching for 30 min, a peak at 99 eV due to elemental silicon from the silicon substrate appears; this is an indication of reduced film thickness.[16] The signal below 101 eV due to elemental silicon was therefore excluded from the analysis. The atomic fractions of Si, C, and O are plotted in Figure 2b. The atomic fraction of C decreases linearly with oxidation time and reaches 4.2% at 40 min, which indicates nearly perfect conversion. The O/Si ratio is 2.4:1, which approximates to that of silicon dioxide and indicates that the PDMS nanodomains have been successfully converted into silica particles that are ordered on the substrate.

We have previously reported a successful fabrication of nanocells in block-copolymer thin films by a process involving supercritical CO_2 ($scCO_2$).[9–12] A thin film of block copolymer with a CO_2-philic block was pressurized with CO_2 to localize it in the CO_2-philic nanodomains. Upon reducing the CO_2 pressure at reduced temperature, the volume of CO_2 in the CO_2-philic domains is converted into voids. In this study, we employ the same methodology with a PS-PDMS block copolymer instead of a fluorinated copolymer to fabricate nanocells in the CO_2-philic PDMS domains.[13]

A PS-PDMS thin film was placed in a high-pressure vessel at 20 MPa and 60 °C for 2 h; the temperature was then reduced isobarically to 0 °C. Subsequently, the pressure was released at a rate of 0.5 MPa min^{-1}. The whole process is the same as that used for the fluorinated block copolymers in our previous study.[9–12] Reducing the temperature to 0 °C freezes the surrounding PS matrix (T_g of PS in 20 MPa of CO_2 is approximately 30 °C)[17] and fixes the morphologies while a significant amount of CO_2 still remains in the PDMS domains. Analytical ellipsometry can be used to measure the thicknesses and refractive indices of the films before and after the CO_2 process, provided that the size of the nanocells is much smaller than the wavelength of light and the effective medium approximation is valid. The increment of thickness, Δd, after the $scCO_2$ process is 4.2 nm from the initial thickness of 43 nm. The porosity is 8.7%, assuming that the film size is fixed in the plane by the substrate and the mass is conserved. The refractive index decreases from 1.56 to 1.50, which corresponds to 9% porosity, according to the Lorentz–Lorenz equation [Eq. (1)].[18] Herein, n_f and n_s are the refractive

$$\frac{n_f^2-1}{n_f^2+2} = (1-V_c)\frac{n_s^2-1}{n_s^2+2} \quad (1)$$

indices of a nanocellular film and a solid skeleton, respectively, and V_c is the porosity. The good agreement between the porosities determined from the thickness and the refractive index indicates the successful introduction of nanocellular structures into the copolymer thin film using this CO_2 process.

This process forms a flat surface with no indication of cellular structures, as confirmed by both scanning electron microscopy (SEM) and AFM. To investigate the structures embedded in the film, reactive ion etching (RIE) with tetrafluoromethane (CF_4) gas was employed to etch the film at a controlled rate.[19,20] An AFM image of the nanocellular structure after 24-nm etching is shown in Figure 3a. The hole pattern in this figure is an evidence of nanocellular structures embedded in the film, as illustrated schematically in Figure 3b. The resulting nanocells have a number density of 7.0×10^{10} cm^{-2} and a spacing of 41.3 nm.

In the last step, nanocellular thin films were fully oxidized by exposure to UV light/ozone for 1 h. Spherical silica dots with an equivalent number density (7.2×10^{10} cm^{-2}) and spacing (40.0 nm) to those of the nanocells in Figure 3a were obtained. An AFM image of these dots, which have an average outer diameter of (29 ± 3) nm, is shown in Figure 3c. If the nanocells in the PDMS domains were still preserved after oxidation, the nanodots should have empty voids (capsules), as illustrated in Figure 3d. To probe the capsule

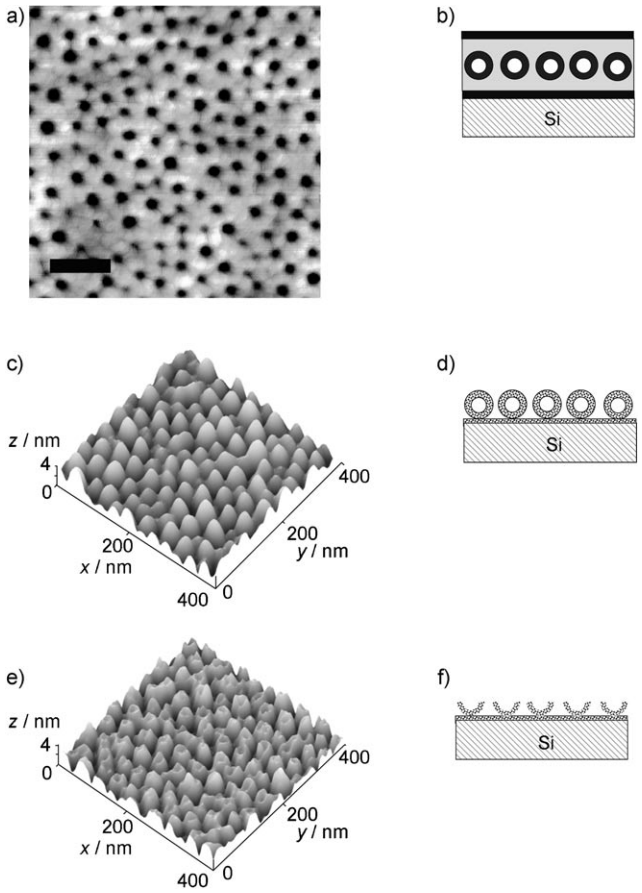

Figure 3. Topographic AFM images and schematic pictures of silica capsules on the substrate. a) Topographic image after RIE for 60 s (scale bar 100 nm), and b) schematic picture of the nanocellular structures on the block-copolymer film. The black and gray domains represent the PDMS and PS domains, respectively; the white part is air. c) Three-dimensional topographic image after oxidation by UV light/ozone, and d) schematic picture of the silica nanocapsules obtained. e) Three-dimensional topographic image after further RIE of 2-nm, and f) schematic picture showing the resulting caldera topography.

structure, the nanodots were etched for 2 min by RIE with a CF_4 rate of 1.5 mL min^{-1} and a powder density of 2 W cm^{-2}. Under these conditions, the etching rate for silica is 1 nm min^{-1}, which means that 2 nm of the silica layer was etched away from the surface. This etching removes the top skin of the capsules and converts them into calderas on the substrate, as shown in Figure 3e and illustrated in Figure 3f. This caldera morphology is clear evidence of a capsule structure before CF_4 etching. The top wall thickness of the silica nanocapsules is approximately 2 nm. The silica capsules were found to be tightly bound to the silicon substrate, even after a long ultrasonic rinse with organic solvents. This successful fabrication of silica nanocapsules provides strong evidence for the presence of CO_2-philic domains surrounding the voids.

In conclusion, we have synthesized silica nanocapsules that are ordered on a substrate by a nondestructive CO_2-foaming method that produces nanocells with the help of a block-copolymer template containing CO_2-philic PDMS domains. The nanocells are formed in the PDMS domains. The PDMS domains surrounding the empty cells are converted into hollow silica particles (nanocapsules) that are ordered on the substrate by oxidation with UV light/ozone. These nanocapsules with a number density of 7.0×10^{10} cm^{-2} have a diameter less than 40 nm and a wall thickness of 2 nm. An advantage of this method over others for the synthesis of nanocapsules is that the nanocapsules are two-dimensionally ordered and controlled using the domain structure of the block-copolymer template. The capsules are easily embedded by deposition after this process. The fabrication of more complex structures using the same method but with different block fractions is currently under investigation.

Experimental Section

A poly(styrene-*b*-dimethylsiloxane) block copolymer was purchased from Polymer Source Inc. The molecular weights of the PS and PDMS blocks are 57600 and 6500 g mol^{-1}, respectively. The silicon wafers were used as received. The PS-PDMS copolymer films were prepared by spin-casting a toluene solution onto silicon substrates. The film thickness was controlled by varying the concentration of the solutions and the rotation speed.

A high-pressure vessel for CO_2 processes was connected to a liquid chromatography pump (JASCO PU-2086 plus) fitted with a cooling head and to a back-pressure regulator (JASCO SCF-Bpg). The PS-PDMS films were placed in the high-pressure vessel at 60 °C for 2 h at a CO_2 pressure of 20 MPa. The vessel was then cooled to 0 °C in an ice bath whilst maintaining the pressure by means of the pump and regulator. The depressurization rate was controlled at 0.5 MPa min^{-1}.

Oxidation of the copolymer thin films by exposure to UV light/ozone was performed in a UVO cleaner 342-101 (Jelight, Inc.). The cleaner generates UV emissions at a wavelength of 254 nm (28 mW cm^{-2}). The distance between the UV source and the silicon wafers was 50 mm.

The film thickness and refractive index were measured with a JASCO M-220 ellipsometer with incident light in a wavelength range of 400–800 nm at an incident angle of 60° with respect to the surface normal. The etching process to expose the embedded cellular structures to the surface and open the hollow spherical structures was performed with a reactive ion etcher (FA-1, SAMCO) and tetrafluoromethane (CF_4) gas. Etching was performed with a CF_4 flow rate of 2 mL min^{-1}, a pressure of 10 Pa, and a power density of 10 W cm^{-2}. The etching rate for PS-PDMS copolymer thin films is approximately 0.4 nm s^{-1} under these conditions.

The surface topography due to the embedded cell structures revealed by RIE was characterized by AFM. AFM measurements were carried out in the tapping mode with an SII SPA300HV. We used a cantilever with a carbon nanotube tip (SII Co.) for the nanocellular PS-PDMS films. Silicon cantilevers (DF-20, SII Co.) were used for the observation of silica nanodots and nanocapsules.

XPS spectra were acquired with a PHI Quantum 2000 spectrometer using monochromated X-rays from an $Al_{K\alpha}$ source with a take-off angle of 45° from the surface plane. The X-ray beam was operating at 20 W and was focused to a diameter of about 100 μm rastered over a 500 μm × 500 μm area. The atomic fractions of carbon, oxygen, and silicon were computed using the attenuation factors provided by the supplier and the sum of these atomic fractions was normalized to unity.

Received: June 7, 2006
Published online: August 25, 2006

Keywords: block copolymers · nanostructures · self-assembly · silica · template synthesis

[1] W. Schartl, *Adv. Mater.* **2000**, *12*, 1899 – 1908.
[2] F. Caruso, *Adv. Mater.* **2001**, *13*, 11 – 22.
[3] a) Z. Z. Yang, Z. W. Niu, Y. F. Lu, Z. B. Hu, C. C. Han, *Angew. Chem.* **2003**, *115*, 1987 – 1989; *Angew. Chem. Int. Ed.* **2003**, *42*, 1943 – 1945; b) E. Bourgeat-Lami, I. Tissot, F. Lefebvre, *Macromolecules* **2002**, *35*, 6185 – 6191; c) F. Caruso, R. A. Caruso, H. Möhwald, *Science* **1998**, *282*, 1111 – 1114.
[4] a) D. Y. Zhao, J. L. Feng, Q. S. Huo, N. Melosh, G. H. Fredrickson, B. F. Chmelka, G. D. Stucky, *Science* **1998**, *279*, 548 – 552; b) N. E. Botterhuis, Q. Y. Sun, P. C. M. M. Magusin, R. A. van Santen, N. A. J. M. Sommerdijk, *Chem. Eur. J.* **2006**, *12*, 1448 – 1456.
[5] M. Yang, J. Ma, C. L. Zhang, Z. Z. Yang, Y. F. Lu, *Angew. Chem.* **2005**, *117*, 6885 – 6888; *Angew. Chem. Int. Ed.* **2005**, *44*, 6727 – 6730.
[6] Y. W. Chen, E. T. Kang, K. G. Neoh, A. Greiner, *Adv. Funct. Mater.* **2005**, *15*, 113 – 117.
[7] M. Lazzari, M. A. Lopez-Quintela, *Adv. Mater.* **2003**, *15*, 1583 – 1594.
[8] C. Park, J. S. Yoon, E. L. Thomas, *Polymer* **2003**, *44*, 6725 – 6760.
[9] H. Yokoyama, L. Li, T. Nemoto, K. Sugiyama, *Adv. Mater.* **2004**, *16*, 1542 – 1546.
[10] L. Li, H. Yokoyama, T. Nemoto, K. Sugiyama, *Adv. Mater.* **2004**, *16*, 1226 – 1229.
[11] H. Yokoyama, K. Sugiyama, *Macromolecules* **2005**, *38*, 10516 – 10522.
[12] L. Li, H. Yokoyama, T. Nemoto, K. Sugiyama, *Macromolecules* **2006**, *39*, 4746 – 4755.
[13] Z. Bayraktar, E. Kiran, *J. Appl. Polym. Sci.* **2000**, *75*, 1397 – 1403.
[14] J. J. Robin, *Adv. Polym. Sci.* **2004**, *167*, 35 – 79.
[15] J. Morvan, M. Camelot, P. Zecchini, C. Roquescarmes, *J. Colloid Interface Sci.* **1984**, *97*, 149 – 156.
[16] J. F. Moulder, W. F. Stickle, P. E. Sobol, K. D. Bomben in *Handbook of X-ray Photoelectron Spectroscopy*, Physical Electronics Inc., Eden Prairie, MN, USA, **1995**, pp. 56 – 57.
[17] W. C. V. Wang, E. J. Kramer, W. H. Sachse, *J. Polym. Sci. Polym. Phys. Ed.* **1982**, *20*, 1371 – 1384.
[18] M. Born, E. Wolf in *Principles of Optics*, Cambridge University Press, Cambridge, UK, **1999**.
[19] H. Yokoyama, T. E. Mates, E. J. Kramer, *Macromolecules* **2000**, *33*, 1888 – 1898.
[20] R. Magerle, *Phys. Rev. Lett.* **2000**, *85*, 2749 – 2752.

